ECOLOGY

# Food web structure for high carbon retention in marine plankton communities

**Hee Chang Kang[1], Hae Jin Jeong[1]*, Jin Hee Ok[1], An Suk Lim[2], Kitack Lee[3], Ji Hyun You[1], Sang Ah Park[1], Se Hee Eom[1], Sung Yeon Lee[1], Kyung Ha Lee[4], Se Hyeon Jang[5], Yeong Du Yoo[6], Moo Joon Lee[7], Kwang Young Kim[5]**



**Total annual net primary productions in marine and terrestrial ecosystems are similar. However, a large portion of the newly produced marine phytoplankton biomass is converted to carbon dioxide because of predation. Which food web structure retains high carbon biomass in the plankton community in the global ocean? In 6954 individual samples or locations containing phytoplankton, unicellular protozooplankton, and multicellular metazooplankton in the global ocean, phytoplankton-dominated bottom-heavy pyramids held higher carbon biomass than protozooplankton-dominated middle-heavy diamonds or metazooplankton-dominated top-heavy inverted pyramids. Bottom-heavy pyramids predominated, but the high predation impact by protozooplankton on phytoplankton or the vertical migration of metazooplankton temporarily changed bottom-heavy pyramids to middle-heavy diamonds or top-heavy inverted pyramids but returned to bottom-heavy pyramids shortly. This finding has profound implications for carbon retention by plankton communities in the global ocean.**



## INTRODUCTION

Before the industrial revolution, Earth's atmosphere contained 280 parts per million (ppm) of carbon dioxide ($CO_2$), equivalent to 600 billion tonnes of carbon (GtC). However, human activities have introduced 300 GtC $CO_2$ (equivalent to a 140-ppm increase) into the atmosphere (*1*–*3*). Approximately 20 to 30% of total anthropogenic $CO_2$ emissions are absorbed by the global ocean, and this process can mitigate global warming (*4*–*6*). The ocean's uptake of anthropogenic $CO_2$ is primarily driven by the difference in $CO_2$ concentrations between the atmosphere and the ocean, which is greatly influenced by rising atmospheric $CO_2$ levels. Marine organisms only directly influence the absorption of anthropogenic $CO_2$ if alterations occur in the quantity of planktonic organic matter that settles to the ocean's depths or in the amount of organic matter retained by marine organisms (*7*).

Total annual net primary production in marine ecosystems (~49 GtC) is similar to that in terrestrial ecosystems (~56 GtC), but the total carbon biomass of all life (i.e., standing stocks) in marine ecosystems is approximately 1% of that in terrestrial ecosystems (*8*, *9*). Most of the newly produced organic matter of primary producers in marine ecosystems is decomposed due to nutrient depletion or predation by predators, mainly zooplankton (*10*). The decomposed organic matter is converted to $CO_2$ by microbes, which sometimes leads to hypoxia (*11*).

Marine phytoplankton account for more than half the carbon biomass of marine photosynthetic organisms (*12*). Unicellular protozooplankton, such as heterotrophic flagellates, ciliates, and amoeboid protists, are major grazers of phytoplankton (*13*–*16*). In general, many marine protozooplankton grow rapidly on phytoplankton but starve to death within a few days, which causes the conversion of organic carbon to $CO_2$ in a short period (*17*). Multicellular metazooplankton, such as rotifers, copepods, and invertebrate larvae, are major predators of protozooplankton (*18*–*21*). They also convert organic carbon to $CO_2$ through respiration during active swimming and feeding on prey (*22*). Thus, feeding by protozooplankton on phytoplankton and metazooplankton on protozooplankton plays a crucial role in the uptake and retention of organic carbon in the ocean. Heterotrophic bacteria are consumed by diverse protozooplankton in a process called the microbial loop (*23*, *24*). Thus, in addition to the transfer of organic carbon from phytoplankton to protozooplankton, that from heterotrophic bacteria to protozooplankton should also be considered.

The carbon biomasses of phytoplankton, protozooplankton, and metazooplankton in an individual sample or location reflect the final production and predation output at a given time. The ratio of carbon biomasses of phytoplankton, protozooplankton, and metazooplankton provides a diverse phytoplankton-based food web structure. If the biomass of phytoplankton is greater than that of protozooplankton, which is greater than that of metazooplankton, then the food web structure is a phytoplankton-dominated bottom-heavy pyramid. If the protozooplankton biomass is greater than that of both phytoplankton and metazooplankton, then the food web structure is a protozooplankton-dominated middle-heavy diamond. If the biomass of metazooplankton is greater than that of protozooplankton, which is greater than that of phytoplankton, then the food web structure is a metazooplankton-dominated top-heavy inverted pyramid. In the phytoplankton plus heterotrophic bacteria–based food webs, the biomasses of phytoplankton and heterotrophic bacteria are summed. Food web structures in marine plankton communities lead to the following critical questions: (i) What is the dominant food web structure in individual plankton

[1]School of Earth and Environmental Sciences, Seoul National University, Seoul 08826, South Korea. [2]Division of Life Science, Gyeongsang National University, Jinju 52828, South Korea. [3]Division of Environmental Science and Engineering, Pohang University of Science and Technology, Pohang 37673, South Korea. [4]Food and Nutrition Tech, CJ CheilJedang, Suwon 16495, South Korea. [5]Department of Oceanography, Chonnam National University, Gwangju 61186, South Korea. [6]Department of Oceanography, Kunsan National University, Kunsan 54150, South Korea. [7]Department of Marine Biotechnology, Anyang University, Incheon 23038, South Korea.
*Corresponding author. Email: hjjeong@snu.ac.kr

samples or locations in the global ocean? (ii) Which food web structure retains high carbon biomass in the plankton community? (iii) Does the food web structure persist in time and space? If not, then what are the mechanisms underlying these changes?

Phytoplankton and protozooplankton can only travel tens of meters per day, whereas metazooplankton can travel hundreds of meters (*25*–*27*). Thus, in the global ocean, it is more reasonable to determine the carbon biomass ratio in individual samples or locations than to estimate the total carbon biomass of phytoplankton compared to that of protozooplankton or metazooplankton.

All available data containing the abundances or carbon biomass of phytoplankton, protozooplankton, and metazooplankton that were found simultaneously in the same individual samples or locations in the global ocean from 1990 to 2021 were analyzed. Using data from these 6954 plankton samples or locations, the phytoplankton-based food web structure and total carbon biomass of each sample or location were determined and the mechanisms that influence them were explored. Furthermore, all available data containing the abundance or carbon biomass of phytoplankton, protozooplankton, metazooplankton, and heterotrophic bacteria found simultaneously in the same individual samples or locations ($n$ = 291), reflecting phytoplankton plus heterotrophic bacteria–based food webs, were analyzed.

## RESULTS AND DISCUSSION

### Types of food web structures in the plankton communities in the global ocean

In the phytoplankton-based food webs, the ratios of phytoplankton, protozooplankton, and metazooplankton biomass in each individual or location sample formed a variety of food web structures (Fig. 1, A and B, figs. S1 to S5, and data S1): bottom-heavy pyramid or triangle (type 1), bottom-wide hourglass (type 2), bottom-wide diamond (type 3), top-wide diamond (type 4), top-wide hourglass (type 5), and top-heavy inverted pyramid or inverted triangle (type 6).

Within the 6954 samples, type 1 constituted the largest proportion (37%), followed by type 3 (26%) (Fig. 1C and table S1). In 51.6% of all individual samples or locations, phytoplankton biomass exceeded total zooplankton biomass (combining protozooplankton and metazooplankton) (Fig. 1D and table S2). Furthermore, in 11 of the 15 regions, types 1 and 2 dominated the food web structure (fig. S6).

In contrast to the findings of the present study, several previous studies have reported that the carbon biomass of heterotrophic plankton is greater than that of phototrophic (autotrophic/mixotrophic) plankton in various marine environments, both locally and globally (*12*, *28*–*30*). Thus, some studies suggested high turnover time as a reason because higher carbon biomass of heterotrophic plankton than phototrophic plankton cannot sustain for a long duration (*12*, *31*). Marine phytoplankton require light and nutrients for photosynthesis; thus, they spend many hours in lit surface water (*32*, *33*). However, surface water is often under conditions of nutrient depletion (*32*). Freshwater input from rivers or large streams after heavy rains temporarily elevates the nutrient concentrations in estuarine and coastal waters (*34*). Fast-growing phytoplankton can bloom by consuming elevated nutrients but die due to nutrient depletion if additional nutrients are not supplied from rivers (*35*). Large quantities of nutrients are stored in deep water (*36*). Upwelling of eutrophic deep waters can increase phytoplankton biomass, but it decreases when the upwelling period ends (*37*). Wind-driven mixing in coastal waters can also temporarily increase the nutrient concentration in surface waters but it does not continue (*38*). Thus, freshwater input after heavy precipitation, upwelling, and mixing in shallow coastal waters during spring and fall can provide high nutrient levels, supporting the high turnover time of phytoplankton. However, these events usually persist for a few days or weeks (*39*, *40*). The results of our analysis suggest that the food web structure in plankton communities is fairly stable and that a high turnover of phytoplankton for a long duration is not necessary.

### Impact of predation changing the food web structure type

In Masan Bay, South Korea, which is internationally known for frequent red tide outbreaks, phytoplankton, protozooplankton, and metazooplankton biomasses in individual samples or locations collected daily from June 2004 to May 2005 fluctuated greatly; the ratio of these three components varied, and the phytoplankton-based food web structure types changed quickly over time (Fig. 2, A and B). The proportion of type 1 was the largest (68%), followed by type 3 (27%), whereas those of types 4, 5, and 6 were almost zero (Fig. 2C). The high predation impact of protozooplankton on the populations of phytoplankton species often changed the food web structure from type 1 to type 3, but the low predation impact did not change the food web structure (Fig. 2, D to F). The changed food web structure returned to the triangular shape within 1 to 8 days (average = ~2 days). The results of laboratory experiments on feeding by diverse protozooplankton species on phytoplankton prey showed that their predation impacts could change phytoplankton dominance to protozooplankton dominance (fig. S7). Therefore, predation can affect the carbon biomass ratio of predators and prey, ultimately altering the food web structure.

Trees are the major primary producers on land and are not easily consumed by animals. Thus, some trees live >1000 years without being consumed by animals (*41*–*43*). However, in the ocean, phytoplankton, which constitute half of the primary producer biomass, are easily consumed by zooplankton (*12*, *44*, *45*). Therefore, the ratio of the carbon biomass of the total primary producers relative to that of animals on land is stable, whereas that in the ocean is temporarily changeable.

### Vertical migration changing the food web structure type

Migratory phytoplankton (mainly flagellates), protozooplankton, and metazooplankton undergo vertical diurnal migration. Migratory phytoplankton and protozooplankton usually migrate over tens of meters between surface and deep waters, staying in surface waters during the day and in deep waters at night (*46*–*48*). Metazooplankton usually migrate hundreds of meters between surface and deeper waters, staying in deeper waters during the day but in surface waters at night (*25*–*27*). In all samples collected from the waters of Southern California of phytoplankton-based food webs, type 2 constituted the largest proportion (48%), followed by type 1 (28%) and type 5 (22%) (Fig. 3, A to C). Types 3, 4, and 6 are rare. The cases of all three depths with types 1 or 2 were 55%, and the upper two depths had types 1 or 2, but the deepest depth with types 5 or 6 was 19% (Fig. 3D and fig. S8). Therefore, they generally predominate at depths where migratory phytoplankton can reach through diurnal vertical migration. However, metazooplankton sometimes predominate in surface or subsurface waters that they reach

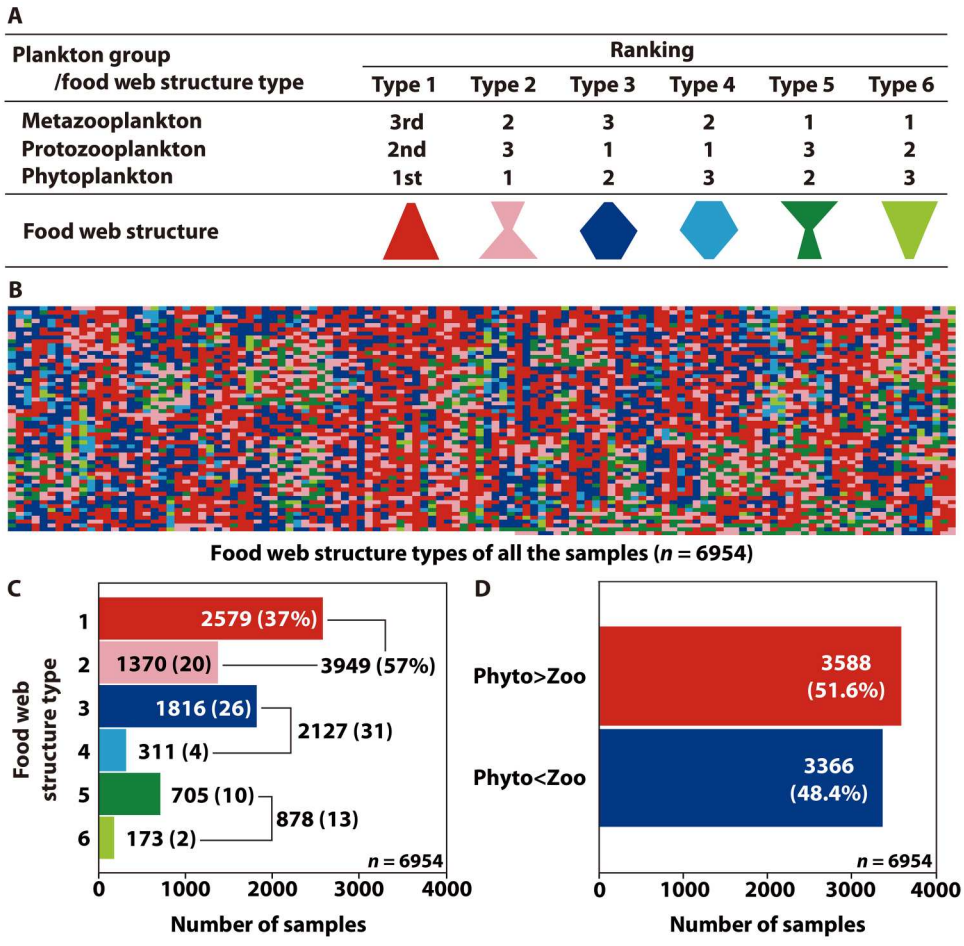


**Fig. 1. Food web structure in the global ocean.** (**A**) Type and color of the phytoplankton-based food web structure classified based on the ranking of the carbon biomass of phytoplankton, protozooplankton, and metazooplankton. (**B**) Heatmap-like image of each type of individual plankton sample or location ($n$ = 6954). (**C**) Number and percentage of the individual samples or locations belonging to each type: phytoplankton-dominant (types 1 and 2), protozooplankton-dominant (types 3 and 4), and metazooplankton-dominant (types 5 and 6). (**D**) Number and percentage of the individual samples or locations in which the carbon biomass of total phytoplankton was greater (phytoplankton > zooplankton) or smaller (phytoplankton < zooplankton) than that of total zooplankton (protozooplankton + metazooplankton).

through diurnal vertical migration. Thus, the food web structure in surface and subsurface waters is changeable because of diurnal vertical migration.

## Food web structure type retaining high carbon biomass

In phytoplankton-based food webs, when summing the carbon biomasses of each group in all the individual samples or locations, those of total phytoplankton, protozooplankton, and metazooplankton were 681,745, 242,538, and 61,786 ng C in a water volume of 6954 ml, respectively (Fig. 4A). Thus, the food web structure of a marine planktonic community is triangular.

When summing the total carbon biomass of each type in all individual samples or locations, type 1 was the highest (636,276 ng C $ml^{-1}$), followed by type 3 (175,337 ng C $ml^{-1}$) (Fig. 4B). Furthermore, type 1 had the highest mean carbon biomass of the three plankton groups (phytoplankton + protozooplankton + metazooplankton) at 247 ng C $ml^{-1}$ (Fig. 4C and table S3). Thus, the triangular food web structure retained the highest carbon biomass.

Among the top 100 ranked samples in terms of total carbon biomass, 92 samples were types 1 or 2, eight samples were type 3, and none were types 4, 5, or 6. Furthermore, the top 43 samples were types 1 or 2, and the sample with the highest total carbon biomass of type 3 was ranked 44th, whereas that of type 5 was ranked 173rd (Fig. 4D). Diatoms, phototrophic nano or microflagellates, and phototrophic dinoflagellates were dominant among the top 43 samples. Thus, the carbon biomass of total plankton in a given water parcel or location may be affected by the food web structure, but not by phytoplankton-dominant groups.

## Phytoplankton plus heterotrophic bacteria–based food web structure

Heterotrophic bacteria usually decompose dead plankton or take up dissolved organic materials and are consumed by protozooplankton (*23*, *24*). Therefore, phytoplankton, heterotrophic bacteria, protozooplankton, and metazooplankton form a food web. By summing phytoplankton and heterotrophic bacteria, additional

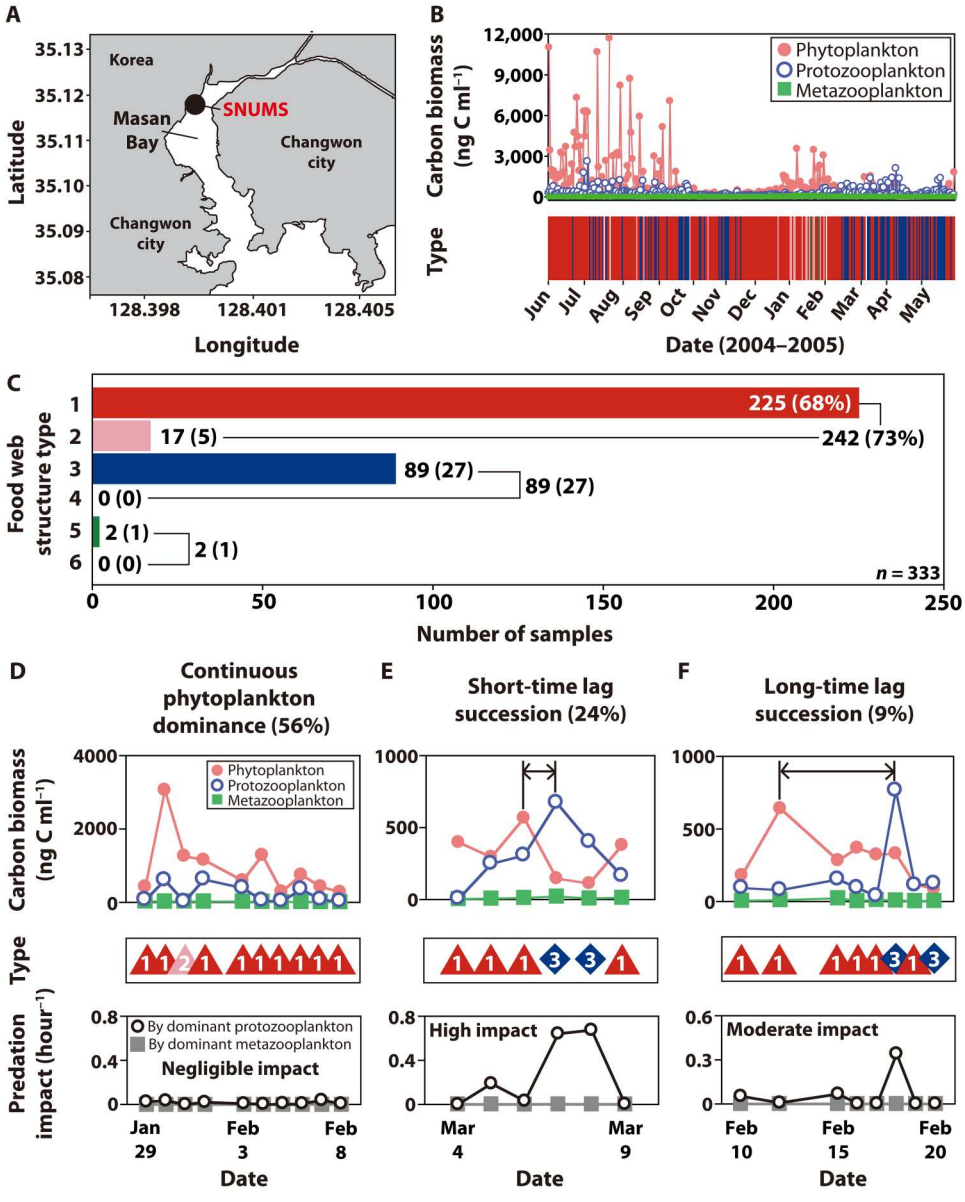


**Fig. 2. Food web structure in Masan Bay and temporal variation.** (**A**) Map of the fixed station [Station SNUMS; redrawn from (*49*)]. (**B**) Variations in phytoplankton, protozooplankton, and metazooplankton biomasses and phytoplankton-based food web structure types from 1 June 2004 to 31 May 2005. (**C**) Number and percentage of the individual samples or locations belonging to each type. (**D** to **F**) Variations in carbon biomass (in ng C $ml^{-1}$) of phytoplankton, protozooplankton, and metazooplankton, types, and predation impact (in $hour^{-1}$) by the dominant protozooplankton (open black circles) and metazooplankton (closed gray squares) on the populations of the dinoflagellate *Prorocentrum cordatum*, the dominant phytoplankton species. Between 29 January and 8 February 2005, phytoplankton continuously dominated due to negligible predation impact (D), between 4 and 9 March 2005, a short-time lag between the phytoplankton and protozooplankton peaks was found because of high predation impact (E), and between 10 February and 20 February 2005, a long time-lag between the phytoplankton and protozooplankton peaks was found because of moderate predation impact (F). The percentage in (D) to (F) is a portion of the number of 10-day periods in which the continuous phytoplankton dominated, the short- or long-time lag occurred for 333 days (i.e., $n = 33$).

six food web structure types PB1, PB2, PB3, PB4, PB5, and PB6 were established.

A total of 291 samples that contained an abundance of phytoplankton, protozooplankton, metazooplankton, and heterotrophic bacteria were available for determining the phytoplankton plus heterotrophic bacteria–based food web types in Masan Bay (Fig. 5). In the phytoplankton plus heterotrophic bacteria–based food web type analyses, type PB1 constituted the largest proportion (80%) and had the highest mean carbon biomass of total plankton (1416 ng C $ml^{-1}$) (Fig. 5, A and B). Phytoplankton plus heterotrophic bacteria–based food webs, when considering both phytoplankton and heterotrophic bacteria as prey for protozooplankton, can support a stable ecosystem at the base of food webs. In the top 20 ranked samples in terms of the total carbon biomass of phytoplankton plus heterotrophic bacteria–based food webs, the carbon biomass

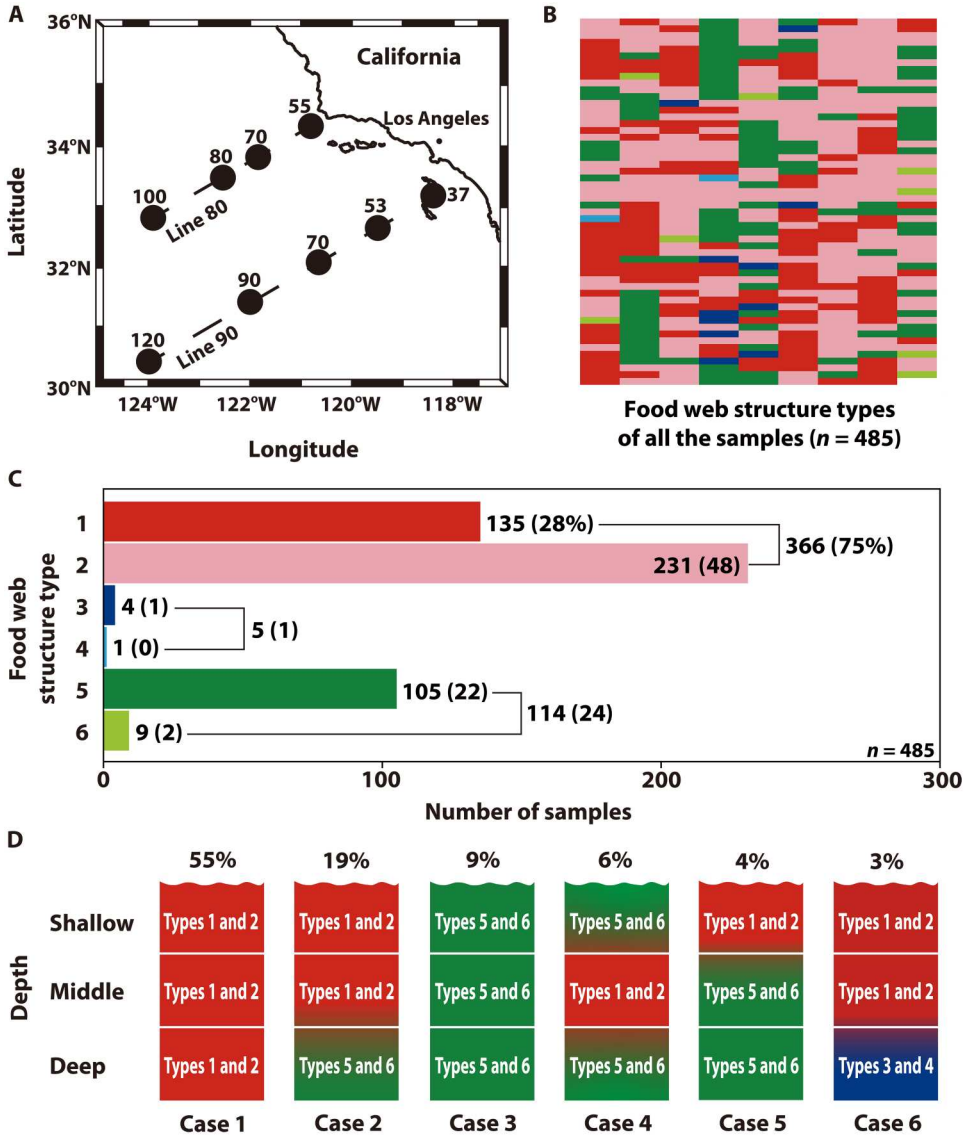


**Fig. 3. Food web structure in Southern California and vertical variation.** (**A**) Map of sampling stations [redrawn from (*51*)]. (**B**) Heatmap-like image of each type of individual samples or locations in the phytoplankton-based food webs ($n$ = 485). (**C**) Number and percentage of the individual samples or locations belonging to each type. (**D**) Percentages of types at three comparative depths (i.e., shallow, middle, and deep) of surface and subsurface waters. In 55% of the samples or locations, phytoplankton dominated at all three depths (types 1 and 2), while in 9%, metazooplankton dominated at all three depths (types 5 and 6).

of heterotrophic bacteria accounted for a small fraction compared with that of phytoplankton (Fig. 5C).

The prevalence of phytoplankton-dominated and phytoplankton plus heterotrophic bacteria–dominated bottom-heavy pyramids (triangles) in marine planktonic communities worldwide carries an important implication for understanding carbon retention by plankton communities and the role of ocean biology in the uptake of oceanic $CO_2$.

## MATERIALS AND METHODS

### Data acquisition on the abundance or carbon biomass of each taxon or group in the plankton communities

To investigate the phytoplankton-based food web structure of plankton communities in the global ocean, all available data containing the abundances or carbon biomasses of phytoplankton (cyanobacteria, diatoms, autotrophic/mixotrophic dinoflagellates, and autotrophic/mixotrophic nano or microflagellates), protozooplankton (heterotrophic dinoflagellates, heterotrophic nano or microflagellates, ciliates, and others), and metazooplankton (copepods, cladocerans, polychaetes, invertebrate larvae, cnidarians, and others) were collected together throughout 1990–2021.

The data of 6954 individual samples or locations were obtained from literature, open-access databases, and our data (table S1); 333

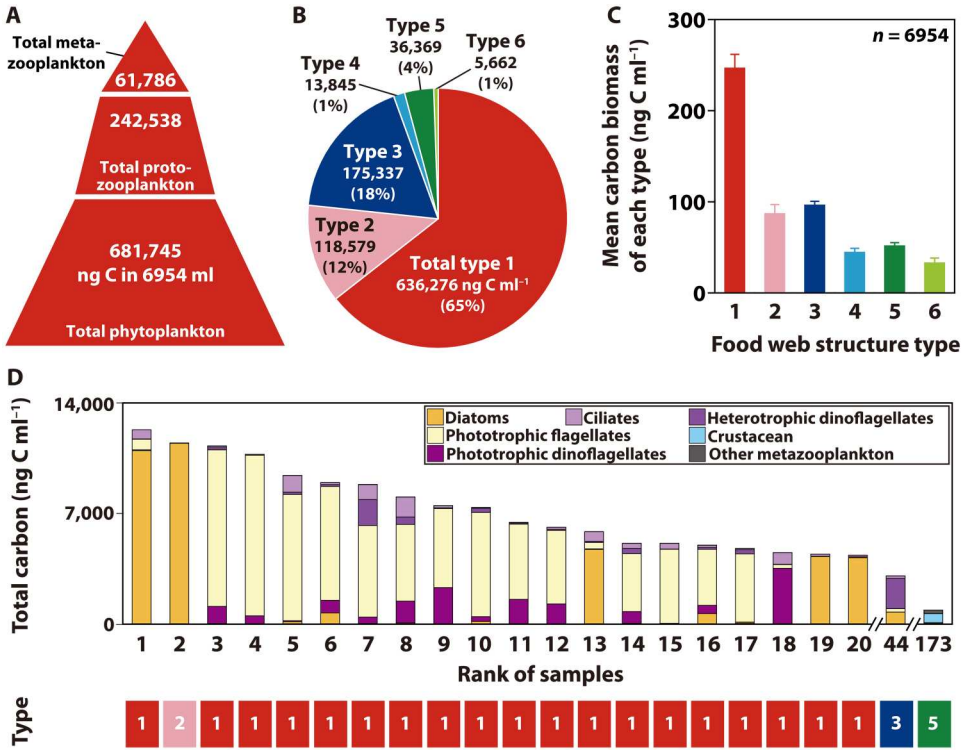


**Fig. 4. Total carbon biomass of each plankton group and the dominant groups in the 20 highest total carbon biomass samples.** (**A** to **C**) Carbon biomasses (in ng C in 6954 ml) of total phytoplankton, protozooplankton, and metazooplankton (A), total carbon biomass (in ng C $ml^{-1}$) of each type (B), and mean carbon biomass (in ng C $ml^{-1}$) of each type (C) in all the individual samples or locations in the phytoplankton-based food webs. Symbols in (C) represent treatment means ± 1 SE. (**D**) Dominant groups and types of samples or locations retaining the top 20 highest carbon biomasses of a total of three plankton groups. In addition, the samples retaining the highest carbon biomasses among types 3 (blue) and 5 (green) ranked in the 44th and 173rd places, respectively.

were collected from coastal waters off Masan, South Korea (*13*, *14*, *49*, *50*), 485 from waters of Southern California, USA, from the Environmental Data Initiative (*51*–*53*), 731 from Australian coastal waters from the Australian Ocean Data Network database (AODN; http://portal.aodn.org.au/) (*54*), 349 from coastal waters off Plymouth, UK, in the western English Channel from the Ocean Biodiversity Information System (*55*–*57*), 52 from the Southern Ocean, Antarctica from the France-Joint Global Ocean Flux Study/Biogeochemical Processes in the Oceans and Fluxes Program (Antares2 and Antares3; www.obs-vlfr.fr/cd_rom_dmtt/start_france_jgofs.htm) (*58*, *59*), 761 from coastal waters off Gwangyang, South Korea, and 4243 from coastal and offshore waters of the South Sea of Korea (*15*, *16*, *60*).

In all samples, except for those collected in Australia, the abundance or carbon biomass of phytoplankton and protozooplankton was analyzed using water samples obtained at various depths. However, for samples collected in Australia, the waters were sampled at the surface and at 10-m-depth intervals, and the samples obtained from each depth were mixed in equal volumes before analysis (*54*). The abundance or carbon biomass of metazooplankton was analyzed using water samples obtained by vertically hauling a net from the target depth or bottom to the surface, as multiple opening/closing nets and environmental sampling system samples were not available.

Some unusually high or low values compared to published papers were screened. Data on environmental factors, such as water temperature, salinity, and nitrate concentrations, were obtained from each source if provided. In addition, to explore the phytoplankton plus heterotrophic bacteria–based food web structure of plankton communities including heterotrophic bacteria, 291 samples containing the abundances or carbon biomasses of phytoplankton, protozooplankton, metazooplankton, and heterotrophic bacteria were analyzed.

## Calculation of the carbon biomass of each plankton group

The carbon biomass of each plankton taxon or group was used as reported in the literature. To determine the carbon biomass of each plankton group, the abundance data were converted into carbon biomass using the following methods: the carbon content of each cultured phytoplankton or protozooplankton taxon was measured using a CHN analyzer (*14*, *49*, *50*), and biovolume was calculated using the width and length of cells in preserved samples that were measured using a light microscope and by considering geometry. The biovolume was converted to carbon content as described in a previous study (*61*). The carbon contents of many other taxa were obtained from the literature. Furthermore, if the phytoplankton abundance is provided as chlorophyll-*a*, then a factor of 40 was used to convert chlorophyll-*a* into carbon (*62*). The carbon content of each phytoplankton and protozooplankton taxon at Plymouth Station L4 in the western English Channel was obtained from the PANGAEA database (*63*, *64*). The carbon content of each metazooplankton taxon was obtained from the literature, if

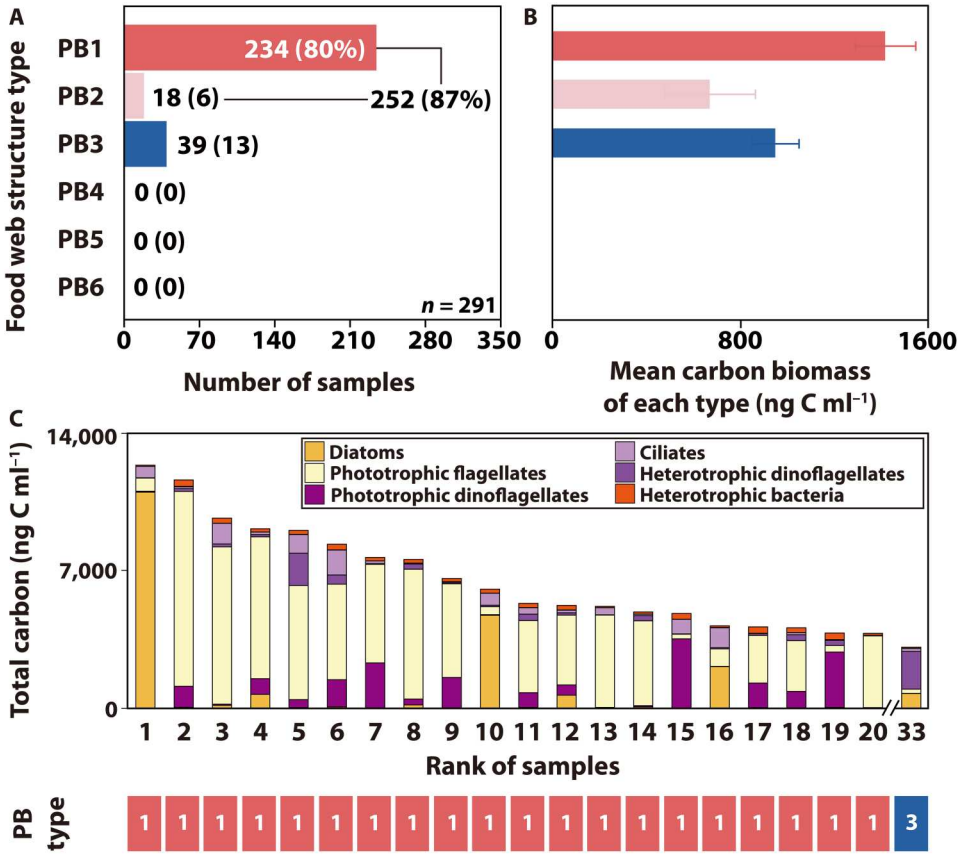


**Fig. 5. Food web structure type and the dominant groups in the phytoplankton plus heterotrophic bacteria–based food webs in Masan Bay.** (**A** and **B**) Number and percentage of individual samples or locations belonging to each type (A) and mean carbon biomass (ng C $ml^{-1}$) of each type in the phytoplankton plus heterotrophic bacteria (PB)–based food webs (B). Symbols represent treatment means ± 1 SE. (**C**) Dominant groups and types of the samples retaining the top 20 highest carbon biomasses of total plankton in the phytoplankton plus heterotrophic bacteria–based food webs. In addition, the samples retaining the highest carbon biomasses among type 3 (blue) ranked in the 33rd place.

reported, or calculated using a factor of 0.2, converting wet to dry weight and 0.5 for converting the dry weight to carbon (*65*). The final unit was unified as ng C $ml^{-1}$. Carbon biomass data of all individual samples used in this study are provided in data S1.

### Classification of food web structure types

The phytoplankton-based food web structure types were classified according to the rank of total phytoplankton, protozooplankton, and metazooplankton carbon biomasses in individual samples or locations (Fig. 1A); type 1 was assigned to the samples with carbon biomasses of phytoplankton > protozooplankton > metazooplankton; type 2 with phytoplankton > metazooplankton > protozooplankton; type 3 with protozooplankton > phytoplankton > metazooplankton; type 4 with protozooplankton > metazooplankton > phytoplankton; type 5 with metazooplankton > phytoplankton > protozooplankton; and type 6 with metazooplankton > protozooplankton > phytoplankton. In phytoplankton plus heterotrophic bacteria–based food webs, phytoplankton and heterotrophic bacteria were summed.

## Supplementary Materials

**This PDF file includes:**
Supplementary Text
Figs. S1 to S8
Tables S1 to S3
Legend for data S1
References

**Other Supplementary Material for this manuscript includes the following:**
Data S1

## REFERENCES AND NOTES

1. N. P. Gillett, M. Kirchmeier-Young, A. Ribes, H. Shiogama, G. C. Hegerl, R. Knutti, G. Gastineau, J. G. John, L. Li, L. Nazarenko, N. Rosenbloom, Ø. Seland, T. Wu, S. Yukimoto, T. Ziehn, Constraining human contributions to observed warming since the pre-industrial period. *Nat. Clim. Change* **11**, 207–212 (2021).
2. S. K. Gulev, P. W. Thorne, J. Ahn, F. J. Dentener, C. M. Domingues, S. Gerland, D. Gong, D. S. Kaufman, H. C. Nnamchi, J. Quaas, J. A. Rivera, S. Sathyendranath, S. L. Smith, B. Trewin, K. von Schuckmann, R. S. Vose, Changing state of the climate system, in *Climate Change 2021: The Physical Science Basis. Contribution of Working Group I to the Sixth Assessment Report of the Intergovernmental Panel on Climate Change*, V. Masson-Delmotte, P. Zhai, A. Pirani, S. L. Connors, C. Péan, S. Berger, N. Caud, Y. Chen, L. Goldfarb, M. I. Gomis, M. Huang, K. Leitzell, E. Lonnoy, J. B. R. Matthews, T. K. Maycock, T. Waterfield, O. Yelekçi, R. Yu, B. Zhou, Eds. (Cambridge Univ. Press, 2021); pp. 287–422.

3. X. Lan, P. Tans, K. W. Thoning, Trends in globally-averaged CO2 determined from NOAA Global Monitoring Laboratory measurements. Version 2023-06 (Global Monitoring Laboratory, 2023).
4. C. L. Sabine, R. A. Feely, N. Gruber, R. M. Key, K. Lee, J. L. Bullister, R. Wanninkhof, C. S. Wong, D. W. R. Wallace, B. Tilbrook, F. J. Millero, T. Peng, A. Kozyr, T. Ono, A. F. Rios, The oceanic sink for anthropogenic $CO_2$. *Science* **305**, 367–371 (2004).
5. C. Le Quéré, M. R. Raupach, J. G. Canadell, G. Marland, L. Bopp, P. Ciais, T. J. Conway, S. C. Doney, R. A. Feely, P. Foster, P. Friedlingstein, K. Gurney, R. A. Houghton, J. I. House, C. Huntingford, P. E. Levy, M. R. Lomas, J. Majkut, N. Metzl, J. P. Ometto, G. P. Peters, I. C. Prentice, J. T. Randerson, S. W. Running, J. L. Sarmiento, U. Schuster, S. Sitch, T. Takahashi, N. Viovy, G. R. van der Werf, F. I. Woodward, Trends in the sources and sinks of carbon dioxide. *Nat. Geosci.* **2**, 831–836 (2009).
6. N. Gruber, D. Clement, B. R. Carter, R. A. Feely, S. van Heuven, M. Hoppema, M. Ishii, R. M. Key, A. Kozyr, S. K. Lauvset, C. L. Monaco, J. T. Mathis, A. Murata, A. Olsen, F. F. Perez, C. L. Sabine, T. Tanhua, R. Wanninkhof, The oceanic sink for anthropogenic $CO_2$ from 1994 to 2007. *Science* **363**, 1193–1199 (2019).
7. K. Lee, Global net community production estimated from the annual cycle of surface water total dissolved inorganic carbon. *Limnol. Oceanogr.* **46**, 1287–1297 (2001).
8. C. B. Field, M. J. Behrenfeld, J. T. Randerson, P. Falkowsk, Primary production of the biosphere: Integrating terrestrial and oceanic components. *Science* **281**, 237–240 (1998).
9. Y. M. Bar-On, R. Phillips, R. Milo, The biomass distribution on Earth. *Proc. Natl. Acad. Sci.* **115**, 6506–6511 (2018).
10. C. M. Duarte, J. Cebrián, The fate of marine autotrophic production. *Limnol. Oceanogr.* **41**, 1758–1766 (1996).
11. D. M. Sigman, M. P. Hain, The biological productivity of the ocean. *Nat. Educ. Knowl.* **3**, 21 (2012).
12. Y. M. Bar-On, R. Milo, The biomass composition of the oceans: A blueprint of our blue planet. *Cell* **179**, 1451–1454 (2019).
13. J. S. Kim, H. J. Jeong, Y. D. Yoo, N. S. Kang, S. K. Kim, J. Y. Song, M. J. Lee, S. T. Kim, J. H. Kang, K. A. Seong, W. H. Yih, Red tides in Masan Bay, Korea, in 2004–2005: III. Daily variations in the abundance of mesozooplankton and their grazing impacts on red-tide organisms. *Harmful Algae* **30**, S102–S113 (2013).
14. Y. D. Yoo, H. J. Jeong, J. S. Kim, T. H. Kim, J. H. Kim, K. A. Seong, S. H. Lee, N. S. Kang, J. W. Park, J. Park, E. Y. Yoon, W. H. Yih, Red tides in Masan Bay, Korea in 2004–2005: II. Daily variations in the abundance of heterotrophic protists and their grazing impact on red-tide organisms. *Harmful Algae* **30**, S89–S101 (2013).
15. M. J. Lee, H. J. Jeong, J. S. Kim, K. K. Jang, N. S. Kang, S. H. Jang, H. B. Lee, S. B. Lee, H. S. Kim, C. H. Choi, Ichthyotoxic *Cochlodinium polykrikoides* red tides offshore in the South Sea, Korea in 2014: III. Metazooplankton and their grazing impacts on red-tide organisms and heterotrophic protists. *Algae* **32**, 285–308 (2017).
16. A. S. Lim, H. J. Jeong, K. A. Seong, M. J. Lee, N. S. Kang, S. H. Jang, K. H. Lee, J. Y. Park, T. Y. Jang, Y. D. Yoo, Ichthyotoxic *Cochlodinium polykrikoides* red tides offshore in the South Sea, Korea in 2014: II. Heterotrophic protists and their grazing impacts on red-tide organisms. *Algae* **32**, 199–222 (2017).
17. H. H. Jakobsen, P. J. Hansen, Prey size selection, grazing and growth response of the small heterotrophic dinoflagellate *Gymnodinium* sp. and the ciliate *Balanion comatum*--a comparative study. *Mar. Ecol. Prog. Ser.* **158**, 75–86 (1997).
18. D. K. Stoecker, J. M. Capuzzo, Predation on protozoa: Its importance to zooplankton. *J. Plankton Res.* **12**, 891–908 (1990).
19. Y. Nakamura, J. T. Turner, Predation and respiration by the small cyclopoid *copepodOithona similisr*: How important is feeding on ciliates and heterotrophic flagellates? *J. Plankton Res.* **19**, 1275–1288 (1997).
20. J. T. Turner, The importance of small planktonic copepods and their roles in pelagic marine food webs. *Zool. Stud.* **43**, 255–266 (2004).
21. S. E. Shumway, J. M. Burkholder, J. Springer, Effects of the estuarine dinoflagellate *Pfiesteria shumwayae* (Dinophyceae) on survival and grazing activity of several shellfish species. *Harmful Algae* **5**, 442–458 (2006).
22. K. B. Heine, A. Abebe, A. E. Wilson, W. R. Hood, Copepod respiration increases by 7% per °C increase in temperature: A meta-analysis. *Limnol. Oceanogr. Lett.* **4**, 53–61 (2019).
23. F. Azam, Microbial control of oceanic carbon flux: The plot thickens. *Science* **280**, 694–696 (1998).
24. D. A. Caron, P. G. Davis, L. P. Madin, J. M. Sieburth, Heterotrophic bacteria and bacterivorous protozoa in oceanic macroaggregates. *Science* **218**, 795–797 (1982).
25. A. S. Brierley, Diel vertical migration. *Curr. Biol.* **24**, R1074–R1076 (2014).
26. M. J. Behrenfeld, P. Gaube, A. D. Penna, R. T. O'Malley, W. J. Burt, Y. Hu, P. S. Bontempi, D. K. Steinberg, E. S. Boss, D. A. Siegel, C. A. Hostetler, P. D. Tortell, S. C. Doney, Global satellite-observed daily vertical migrations of ocean animals. *Nature* **576**, 257–261 (2019).
27. K. Bandara, Ø. Varpe, L. Wijewardene, V. Tverberg, K. Eiane, Two hundred years of zooplankton vertical migration research. *Biol. Rev.* **96**, 1547–1589 (2021).
28. Q. Dortch, T. T. Packard, Differences in biomass structure between oligotrophic and eutrophic marine ecosystems. *Deep Sea Res. Part A. Oceanogr. Res. Pap.* **36**, 223–240 (1989).
29. J. M. Gasol, P. A. Del Giorgio, C. M. Duarte, Biomass distribution in marine planktonic communities. *Limnol. Oceanogr.* **42**, 1353–1363 (1997).
30. E. T. Buitenhuis, M. Vogt, R. Moriarty, N. Bednaršek, S. C. Doney, K. Leblanc, C. Le Quéré, Y. -W. Luo, C. O'Brien, T. O'Brien, J. Peloquin, R. Schiebel, C. Swan, MAREDAT: Towards a world atlas of MARine Ecosystem DATa. *Earth Syst. Sci. Data* **5**, 227–239 (2013).
31. D. J. McCauley, G. Gellner, N. D. Martinez, R. J. Williams, S. A. Sandin, F. Micheli, P. J. Mumby, K. S. McCann, On the prevalence and dynamics of inverted trophic pyramids and otherwise top-heavy communities. *Ecol. Lett.* **21**, 439–454 (2018).
32. L. A. Bristow, W. Mohr, S. Ahmerkamp, M. M. Kuypers, Nutrients that limit growth in the ocean. *Curr. Biol.* **27**, R474–R478 (2017).
33. A. Burson, M. Stomp, E. Greenwell, J. Grosse, J. Huisman, Competition for nutrients and light: Testing advances in resource competition with a natural phytoplankton community. *Ecology* **99**, 1108–1118 (2018).
34. T. D. Jickells, Nutrient biogeochemistry of the coastal zone. *Science* **281**, 217–222 (1998).
35. J. E. Cloern, Phytoplankton bloom dynamics in coastal ecosystems: A review with some general lessons from sustained investigation of San Francisco Bay, California. *California. Rev. Geophys.* **34**, 127–168 (1996).
36. X. Zhang, B. B. Ward, D. M. Sigman, Global nitrogen cycle: Critical enzymes, organisms, and processes for nitrogen budgets and dynamics. *Chem. Rev.* **120**, 5308–5351 (2020).
37. F. P. Wilkerson, A. M. Lassiter, R. C. Dugdale, A. Marchi, V. E. Hogue, The phytoplankton bloom response to wind events and upwelled nutrients during the CoOP WEST study. *Deep Sea Res. Part II Top. Stud. Oceanogr.* **53**, 3023–3048 (2006).
38. J. U. Wihsgott, J. Sharples, J. E. Hopkins, E. M. S. Woodward, T. Hull, N. Greenwood, D. B. Sivyer, Observations of vertical mixing in autumn and its effect on the autumn phytoplankton bloom. *Prog. Oceanogr.* **177**, 102059 (2019).
39. C. Aguirre, R. Garreaud, L. Belmar, L. Farías, L. Ramajo, F. Barrera, High-frequency variability of the surface ocean properties off central Chile during the upwelling season. *Front. Mar. Sci.* **8**, 702051 (2021).
40. A. Comesaña, B. Fernández-Castro, P. Chouciño, E. Fernández, A. Fuentes-Lema, M. Gilcoto, M. Pérez-Lorenzo, B. Mouriño-Carballido, Mixing and phytoplankton growth in an upwelling system. *Front. Mar. Sci.* **8**, 712342 (2021).
41. A. Lara, R. Villalba, A 3620-year temperature record from *Fitzroya cupressoides* tree rings in southern South America. *Science* **260**, 1104–1106 (1993).
42. M. Blicharska, G. Mikusiński, Incorporating social and cultural significance of large old trees in conservation policy. *Conserv. Biol.* **28**, 1558–1567 (2014).
43. A. Black, N. Waipara, M. Gerth, Calling time on New Zealand's oldest tree species. *Nature* **561**, 177 (2018).
44. H. J. Jeong, Y. D. Yoo, J. S. Kim, K. A. Seong, N. S. Kang, T. H. Kim, Growth, feeding and ecological roles of the mixotrophic and heterotrophic dinoflagellates in marine planktonic food webs. *Ocean Sci. J.* **45**, 65–91 (2010).
45. D. K. Steinberg, M. R. Landry, Zooplankton and the ocean carbon cycle. *Ann. Rev. Mar. Sci.* **9**, 413–444 (2017).
46. T. Shikata, S. Matsunaga, H. Nishide, S. Sakamoto, G. Onistuka, M. Yamaguchi, Diurnal vertical migration rhythms and their photoresponse in four phytoflagellates causing harmful algal blooms. *Limnol. Oceanogr.* **60**, 1251–1264 (2015).
47. S. Lovecchio, E. Climent, R. Stocker, W. M. Durham, Chain formation can enhance the vertical migration of phytoplankton through turbulence. *Sci. Adv.* **5**, eaaw7879 (2019).
48. K. Wirtz, S. L. Smith, M. Mathis, J. Taucher, Vertically migrating phytoplankton fuel high oceanic primary production. *Nat. Clim. Change* **12**, 750–756 (2022).
49. H. J. Jeong, Y. D. Yoo, K. H. Lee, T. H. Kim, K. A. Seong, N. S. Kang, S. Y. Lee, J. S. Kim, S. Kim, W. H. Yih, Red tides in Masan Bay, Korea in 2004–2005: I. Daily variations in the abundance of red-tide organisms and environmental factors. *Harmful Algae* **30**, S75–S88 (2013).
50. H. J. Jeong, Y. D. Yoo, K. Lee, H. C. Kang, J. S. Kim, K. Y. Kim, Annual carbon retention of a marine-plankton community in the eutrophic Masan Bay, based on daily measurements. *Mar. Biol.* **168**, 1–10 (2021).
51. K. M. Kenitz, A. W. Visser, M. D. Ohman, M. R. Landry, K. H. Andersen, Community trait distribution across environmental gradients. *Ecosystems* **22**, 968–980 (2019).
52. California Current Ecosystem LTER, M. Landry, Size group (pico, nano, micro) and group total carbon estimates from cell counts via epifluorescent microscopy (EPI) of heterotrophic and autotrophic plankton from CCE-CalCOFI Augmented cruises in the California Current System, 2004–2011 (ongoing), version 3 (Environmental Data Initiative, 2017).
53. California Current Ecosystem LTER, M. Landry, Picophytoplankton and bacteria total carbon estimates from cell counts analyzed with flow cytometry (FCM) from CCE-CalCOFI Augmented cruises in the California Current System, 2004–2019 (ongoing), version 6 (Environmental Data Initiative, 2019).
54. R. S. Eriksen, C. H. Davies, P. Bonham, F. E. Coman, S. Edgar, F. R. McEnnulty, D. McLeod, M. J. Miller, W. Rochester, A. Slotwinski, M. L. Tonks, J. Uribe-Palomino, A. J. Richardson,

Australia's long-term plankton observations: The integrated marine observing system national reference station network. *Front. Mar. Sci.* **6**, 161 (2019).
55. D. Eloire, P. J. Somerfield, D. V. Conway, C. Halsband-Lenk, R. Harris, D. Bonnet, Temporal variability and community composition of zooplankton at station L4 in the Western Channel: 20 years of sampling. *J. Plankton Res.* **32**, 657–679 (2010).
56. C. E. Widdicombe, D. Eloire, D. Harbour, R. P. Harris, P. J. Somerfield, Long-term phytoplankton community dynamics in the Western English Channel. *J. Plankton Res.* **32**, 643–655 (2010).
57. T. J. Smyth, J. R. Fishwick, L. AL-Moosawi, D. G. Cummings, C. Harris, V. Kitidis, A. Rees, V. Martinez-Vicente, E. M. S. Woodward, A broad spatio-temporal view of the Western English Channel observatory. *J. Plankton Res.* **32**, 585–601 (2010).
58. S. Becquevort, P. Menon, C. Lancelot, Differences of the protozoan biomass and grazing during spring and summer in the Indian sector of the Southern Ocean. *Polar Biol.* **23**, 309–320 (2000).
59. P. Mayzaud, V. Tirelli, A. Errhif, J. P. Labat, S. Razouls, R. Perissinotto, Carbon intake by zooplankton. Importance and role of zooplankton grazing in the Indian sector of the Southern Ocean. *Deep-Sea Res. II Top. Stud. Oceanogr.* **49**, 3169–3187 (2002).
60. H. J. Jeong, A. S. Lim, K. Lee, M. J. Lee, K. A. Seong, N. S. Kang, S. H. Jang, K. H. Lee, S. Y. Lee, M. O. Kim, J. H. Kim, J. E. Kwon, H. C. Kang, J. S. Kim, W. Yih, K. Shin, P. K. Jang, J. -H. Ryu, S. Y. Kim, J. Y. Park, K. Y. Kim, Ichthyotoxic *Cochlodinium polykrikoides* red tides offshore in the South Sea, Korea in 2014: I. Temporal variations in three-dimensional distributions of red-tide organisms and environmental factors. *Algae* **32**, 101–130 (2017).
61. S. Menden-Deuer, E. J. Lessard, Carbon to volume relationships for dinoflagellates, diatoms, and other protist plankton. *Limnol. Oceanogr.* **45**, 569–579 (2000).
62. D. H. Peterson, J. F. Festa, Numerical simulation of phytoplankton productivity in partially mixed estuaries. *Estuar. Coast. Shelf Sci.* **19**, 563–589 (1984).
63. C. E. Widdicombe, D. Eloire, D. Harbour, R. P. Harris, P. J. Somerfield, Time series of phytoplankton abundance and composition at station L4 in the English Channel from 1988 to 2009 (PANGAEA, 2010).
64. C. E. Widdicombe, D. Eloire, D. Harbour, R. P. Harris, P. J. Somerfield, Time series of microzooplankton abundance and composition at station L4 in the English Channel from 1988 to 2009 (PANGAEA, 2010).
65. M. Omori, Weight and chemical composition of some important oceanic zooplankton in the North Pacific Ocean. *Mar. Biol.* **3**, 4–10 (1969).
66. R. C. Hooff, W. T. Peterson, Copepod biodiversity as an indicator of changes in ocean and climate conditions of the northern California current ecosystem. *Limnol. Oceanogr.* **51**, 2607–2620 (2006).
67. S. Chiba, S. D. Batten, T. Yoshiki, Y. Sasaki, K. Sasaoka, H. Sugisaki, T. Ichikawa, Temperature and zooplankton size structure: Climate control and basin-scale comparison in the North Pacific. *Ecol. Evol.* **5**, 968–978 (2015).
68. A. Atkinson, Life cycles of *Calanoides acutus*, *Calanus simillimus* and *Rhincalanus gigas* (Copepoda: Calanoida) within the Scotia Sea. *Mar. Biol.* **109**, 79–91 (1991).
69. H. J. Jeong, J. Y. Yoon, J. S. Kim, Y. D. Yoo, K. A. Seong, Growth and grazing rates of the prostomatid ciliate *Tiarina fusus* on red-tide and toxic algae. *Aquat. Microb. Ecol.* **28**, 289–297 (2002).
70. H. C. Kang, H. J. Jeong, S. J. Kim, J. H. You, J. H. Ok, Differential feeding by common heterotrophic protists on 12 different *Alexandrium* species. *Harmful Algae* **78**, 106–117 (2018).
71. S. A. Park, H. J. Jeong, J. H. Ok, H. C. Kang, J. H. You, S. H. Eom, E. C. Park, Interactions between the kleptoplastidic dinoflagellate *Shimiella gracilenta* and several common heterotrophic protists. *Front. Mar. Sci.* **8**, 738547 (2021).
72. M. D. Johnson, The acquisition of phototrophy: Adaptive strategies of hosting endosymbionts and organelles. *Photosynth. Res.* **107**, 117–132 (2011).
73. J. H. Ok, H. J. Jeong, H. C. Kang, S. A. Park, S. H. Eom, J. H. You, S. Y. Lee, Ecophysiology of the kleptoplastidic dinoflagellate *Shimiella gracilenta*: I. Spatiotemporal distribution in Korean coastal waters and growth and ingestion rates. *Algae* **36**, 263–283 (2021).
74. R. Harris, C. Widdicombe, L4 plankton monitoring programme (Plymouth Marine Laboratory, 2007).

**Acknowledgments:** We thank N. S. Kang, J. S. Kim, and K. A. Seong for technical support and M. Ohman and K. Kenitz for sharing data on plankton in the waters off Southern California.
**Funding:** This work was supported by the National Research Foundation funded by the Ministry of Science and ICT NRF-2021M3I6A1091272 (to H.J.J.), the National Research Foundation funded by the Ministry of Science and ICT NRF-2021R1A2C1093379 (to H.J.J.), the Korea Institute of Marine Science & Technology Promotion funded by the Ministry of Oceans and Fisheries 20230018 (to H.J.J.). **Author contributions:** Conceptualization: H.C.K. and H.J.J. Methodology: H.C.K. and H.J.J. Investigation: H.C.K., H.J.J., J.H.O., A.S.L., J.H.Y., S.A.P., S.H.E., S.Y.L., K.H.L., S.H.J., Y.D.Y., and M.J.L. Visualization: H.C.K. and H.J.J. Funding acquisition: H.J.J. Project administration: H.J.J. Supervision: H.J.J. Writing—original draft: H.C.K., H.J.J., K.L., and K.Y.K. Writing—review and editing: H.C.K. and H.J.J. **Competing interests:** The authors declare that they have no competing interests. **Data and materials availability:** Data on the carbon biomass of phytoplankton and protozooplankton in the waters off Southern California were obtained from the Environmental Data Initiative [EDI; (*52*, *53*)]. Data on the abundance and biovolume of plankton in Australian coastal waters were obtained from Australia's Integrated Marine Observing System (IMOS) which is enabled by the National Collaborative Research Infrastructure Strategy (NCRIS) available at Open Access to Ocean Data (AODN, https://portal.aodn.org.au/). Data on plankton abundance in the western English Channel were obtained from the Ocean Biodiversity Information System [OBIS; (*74*)]. Data on the carbon contents of each phytoplankton and protozooplankton species in the western English Channel were obtained from PANGAEA (*63*, *64*). Data on the abundance or carbon biomass of plankton in the Southern Ocean, Antarctica were obtained from the France-JGOFS/PROOF Program (Antares2 and Antares3; http://www.obs-vlfr.fr/cd_rom_dmtt/start_france_jgofs.htm). All data needed to evaluate the conclusions in the paper are present in the paper and/or the Supplementary Materials.

Submitted 1 August 2023
Accepted 15 November 2023
Published 15 December 2023
10.1126/sciadv.adk0842